UNCLASSIFIED

AD 296 312

Reproduced by the

ARMED SERVICES TECHNICAL INFORMATION AGENCY
ARLINGTON HALL STATION
ARLINGTON 12, VIRGINIA

UNCLASSIFIED

NOTICE: When government or other drawings, specifications or other data are used for any purpose other than in connection with a definitely related government procurement operation, the U. S. Government thereby incurs no responsibility, nor any obligation whatsoever; and the fact that the Government may have formulated, furnished, or in any way supplied the said drawings, specifications, or other data is not to be regarded by implication or otherwise as in any manner licensing the holder or any other person or corporation, or conveying any rights or permission to manufacture, use or sell any patented invention that may in any way be related thereto.

296 312
296 312
AD No. ____
ASTIA FILE COPY

FIRST QUARTERLY REPORT

THIN FILM ACTIVE DEVICES

22 June to 22 September 1962

James P. Spratt

Contract No. DA-49-186-ORD-1056
with
Diamond Ordnance Fuze Laboratories

ASTIA
FEB 19 1963
TISIA

PHILCO
A SUBSIDIARY OF Ford Motor Company
SCIENTIFIC LABORATORY

$4.60

Copy No. ____________

FIRST QUARTERLY REPORT

THIN FILM ACTIVE DEVICES

22 June to 22 September 1962

James P. Spratt

Contract No. DA-49-186-ORD-1056
with
Diamond Ordnance Fuze Laboratories

22 October 1962

PHILCO
A SUBSIDIARY OF Ford Motor Company
SCIENTIFIC LABORATORY
BLUE BELL, PENNSYLVANIA

TABLE OF CONTENTS

TABLE OF CONTENTS (contd)

LIST OF ILLUSTRATIONS

LIST OF TABLES

SECTION I

PURPOSE

This is the First Quarterly Report, covering the period 22 June to 22 September 1962, on Contract No. DA-49-186-ORD-1056 with Diamond Ordnance Fuze Laboratories for work on Thin Film Active Devices.

The purpose of this work is to conduct a research and development program directed toward the development of an active thin film triode device dependent upon tunneling for its gain mechanism. This program will be carried out in such a way to allow the early fabrication of thin film triodes, the extension and refinement of thin film techniques related to fabrication, and the extension and refinement of the theoretical understanding of these devices.

Reviewed and transmitted
for Philco Corporation by

Carlo V. Bocciarelli /ASW

Carlo V. Bocciarelli
Associate Director of Research
Basic Science and Technology Dept.

SECTION II

ABSTRACT

The problem of collecting hot electrons from a metal by means of a simple metal-insulator interface is discussed. Backscattering out of the insulator is shown to be a serious problem if high collection efficiencies ~~(≈ 1)~~ are desired.

Fabrication of tunnel emitters for the Metal Edge Amplifier (MEA) was seriously hindered by shorting through the natural oxide of aluminum. A more fundamental examination of the oxidation process was begun and, in the meantime, attempts will be made to use evaporated insulators for device fabrication.

SECTION III

PUBLICATIONS, LECTURES, REPORTS AND CONFERENCES

No papers were published, lectures given, or reports written concerning the work of this contract during the period covered by this report.

The following conference was held:

Date: 22 August 1962

Place: Diamond Ordnance Fuze Laboratories, Washington, D. C.

Organizations: D.O.F.L., N.A.S.A., and Philco

Participants: Messrs. T. Liimatainen, J. Scales, Q. Kaiser, O. Meyer,
C. Klute, and P. Landis of D.O.F.L.
J. Walker of N.A.S.A.
R. A. Williams and J. P. Spratt of Philco Scientific Laboratory.

Subjects Discussed: Background and current status work on contract.

SECTION IV

FACTUAL DATA

A. Introduction

The very severe conditions imposed on electronic systems for use in space environments have resulted in an extensive evaluation of new active device mechanisms which might meet these conditions. This evaluation has resulted in the conclusion that a thin film device utilizing metals and insulators, rather than a device employing single-crystal semiconductors, would be superior to existing solid state devices in temperature insensitivity and radiation resistance. Furthermore, such devices would be more compatible with microelectronic systems, since they would not require single-crystal materials. Two device mechanisms applicable in principle to thin film structures, have recently come to light,[1,2,3] both of which are majority carrier effects utilizing tunnel injection. The tunneling process is known to be temperature insensitive, and is an excellent choice for structures designed to encounter severe environmental conditions. The purpose of this program is to study and develop these two gain mechanisms so that a thin film triode can be produced which will offer substantial improvement over conventional solid state devices in radiation resistance.

The two device mechanisms under study are the tunnel emission hot electron device as suggested by Mead,[1] and the controlled internal field emission device.[2] These two effects will be described below, and the present state of theoretical understanding and the state of the art in fabrication of such devices presented.

1. Basic Concepts of Hot Electron Devices

The concept of the hot electron device is based upon the ability to transport through a metal film electrons having an energy in excess of the equilibrium energy; hence the term "hot" electrons. It has been shown[4,5,6] that energetic electrons can travel substantial distances in metals before their excess energy is lost by collisions. Thus, a thin metal film can be made to act as a coupler between a low impedance source and a high impedance sink of energetic electrons. In this respect, such a device is similar to a bipolar transistor where, due to the long paths for minority carriers in single-crystal germanium and silicon, a layer of these semiconductors provides coupling between a low impedance source and a high impedance sink. Thus, a fundamental problem in the design of hot carrier devices is that of mean free path of electrons in metal films. Spitzer et al[6] have shown the "effective transport distance" L in gold to be 740 Å. Berman[5] has shown that the condition that must be met in a device is

$$t << L = \left[\frac{1}{3} \ \ell_e \ell_p \right]^{1/2} \tag{1}$$

where

t = the thickness of the base metal film

ℓ_e = the mean free path between electron-electron collisions

ℓ_p = the mean free path between electron-phonon collisions.

Philco currently is sponsoring an in-house program to determine values of L for a wide range of film materials evaporated under ultra-high vacuum conditions. The results of this program will allow judicious selection of base film materials, thereby allowing work under this contract to be concentrated on the emitter and collector barrier materials.

a. Emission of Hot Electrons into a Metal by Tunneling

The second basic problem in hot electron devices is that of creating (or injecting) the hot electrons. The use of electron tunneling through a thin barrier as a means of injecting hot electrons into a metal film has been under study at Philco Scientific Laboratory for some time. While other methods of hot electron injection have been suggested,[7,8,9] tunneling still appears most promising for an all-thin-film, hot-electron device. The requirements which must be met by an emitter are that it be:

(i) Of low impedance,

(ii) an efficient source of essentially monoenergetic hot electrons, and

(iii) capable of high current densities.

That these conditions can, at least theoretically, be met by a tunneling structure can be shown by an examination of the I-V characteristics predicted for a tunnel barrier.[10]

(1) Direct Metal-to-Metal Tunneling

When the potential difference V across a metal-insulator-metal sandwich is less than the barrier height ϕ, between the metal and the insulator, electrons tunnel directly from metal-to-metal. In this case, it can be shown that the current-voltage characteristic at $0^{o}K$ is given by [10]

$$J = \frac{4\pi m_o^* q}{h^3} \quad W_{1/e}^{\ 1/2} \left(\exp \ \frac{2\phi_1}{W_{1/e}} \right) \left[1\text{-}\exp \ - \ \frac{V}{W_{1/e}} \right] \tag{2}$$

where

$W_{1/e}$ = the half width of the electron energy distribution about a center energy of $q \ V_{EB}$.

$$W_{1/e} = \left[\frac{\hbar^2}{2 \ m_o^*} \right]^{1/2} \frac{\phi_1^{\ 1/2}}{a_o \left[1 + \frac{1}{4} \quad \frac{V_o + V}{\phi_1} \right]} \tag{3}$$

where V = applied voltage
ϕ_1 = metal-insulator barrier height
a_o = the thickness of the insulator

V_o = the built-in voltage across the insulator

m_o^* = the effective electron mass in the insulator.

(2) Fowler-Nordheim Tunneling

In the high bias case; i.e., when $V > \phi_1$, the current-voltage characteristic approaches that given by Fowler and Nordheim [11]

$$J = \frac{4\pi m_o^* q}{h^3} \quad W_{1/e}^2 \quad \exp \left(- \frac{2}{3} \quad \frac{\phi_1}{W_{1/e}} \right) \tag{4}$$

where here

$$W_{1/e} = \left[\frac{\hbar^2}{8 \ m_o^*} \right]^{1/2} \frac{V_o + V}{a_o \ \phi_1^{1/2}} \ . \tag{5}$$

(3) Practical Tunnel Emitters

The above equations show the importance of achieving high fields in the emitter barrier, since the current density that can be passed by a tunnel junction depends exponentially on field strength, E. Several programs are underway at Philco to study various thin insulator films which may give high values of E_{MAX}, emitter breakdown. One of the insulators being studied as part of this program is the natural oxide of aluminum.

b. Collection of Hot Electrons

After high energy electrons are injected into and transported across the base film, the final problem is one of collection. A preliminary expression for the current collected at a metal-insulator, or metal-semiconductor interface is

$$I_c \sim \int_{\phi_1}^{V_{EB}} \delta(E)\ V(E)\ F(E)\ dE \tag{6}$$

where

V_{EB} = emitter-base voltage

$\delta(E)$ = electron density injected into base

$V(E)$ = reflection factor at base collector interface

$F(E)$ = loss function, representing changes in electron energy distribution caused by scattering in the base.

This equation shows the importance of achieving low values of ϕ_c, since if $\phi_c \geq V_{EB}$, $I_c = 0$. Since V_{EB} is limited by the maximum field strength in the emitter barrier, it is desirable to have a low value of ϕ_c. One of the theoretical tasks of this contract is to evaluate the reflection factor V(E), and determine its dependence on ϕ_c and $V_{EB}-\phi_c$. Such an analysis is presented in Part B, "Theoretical Analysis."

c. Summary

The feasibility of using hot electron transport in metals as the basis of a new solid state active triode, as suggested by Mead,[1] has been verified in structures using single-crystal collectors.[2,12,13] Still unresolved however, are the questions concerning the maximum current gains (α_{CB}) which can be obtained with hot electron devices, and the feasibility of producing all-film versions of such structures. A parallel program* is currently underway at Philco to study the applicability of films of high gap semiconductors, such as cadmium sulfide and zinc sulfide, as collectors in tunnel emission hot electron structures. The program reported on here will concern itself with determining maximum current gains obtainable in metal-insulator versions of this structure, and a study of problems associated with fabricating metal-insulator triodes.

2. Basic Concepts of the Controlled Internal Field Emission Device

Out of Philco's study of thin-film, tunnel emission devices has evolved a new gain mechanism utilizing controlled tunneling. This effect[3] relies on the ability of a control electrode to modulate tunneling occurring between two other electrodes without itself taking part in the tunneling. This process is best described by considering the geometry shown in Figure 1. When this structure is biased as shown, a high field is established in the insulator between the two metals. This field will fringe over into the semiconductor, so that the maximum field in the semiconductor is given by[3]

$$E^2_{MAX} \approx E^2_{EB} + E^2_{EC} \tag{7}$$

where

E_{EB} = the field in the insulator

E_{EC} = the field between emitter and collector far from the edge.

For a semiconductor doped to concentration N_D,[3]

$$E^2_{MAX} \approx \frac{V^2_{EB}}{d^2} + \frac{2\, q\, N_D}{K} V_{CE} \tag{8}$$

where

V_{EB} = emitter-base bias voltage

d = insulator thickness (assumed uniform)

k = the dielectric constant of the semiconductor

V_{CE} = the emitter-collector bias voltage.

---

* Signal Corps Contract No. DA-36-039-SC-90715, USASRDL, Fort Monmouth, N.J.

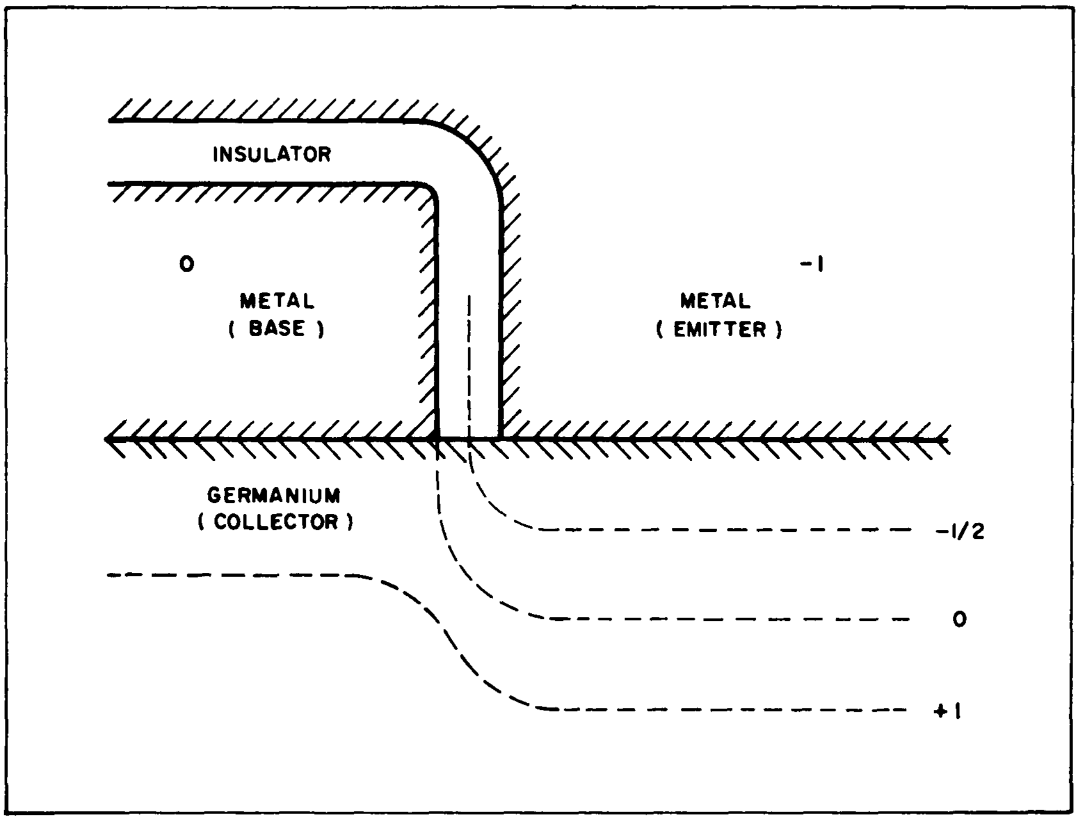

FIGURE 1 CROSS SECTIONAL VIEW OF EDGE-EFFECT DEVICE

If E_{MAX} is high enough to cause tunneling in the semiconductor, and yet low enough that the emitter base impedance is still high, then a current I_g will flow in the emitter-to-collector loop which is a strong function of E^2_{MAX}. Thus,

$$I_g = f(E^2_{MAX}). \tag{9}$$

The small signal current which results is given by

$$i_g = \frac{df}{d\,E^2_{MAX}} \left[\frac{\partial\, E^2_{MAX}}{\partial\, V_{EC}}\, v_{EB} - \frac{2\, E^2_{MAX}}{2\, V_{EC}}\, v_{EC} \right] \tag{10}$$

$$= \frac{df}{d\,E^2_{MAX}} \left[\frac{2\, V_{EB}}{d^2}\, v_{EB} \quad \frac{2\,q\,N_D}{K}\, v_{EC} \right] \tag{11}$$

(sign of v_{EC} has been reversed from that of V_{EC} to conform with convention)

$$\therefore\ i_g = g_o\, v_{EB} - g_o\, \mu_o\, v_{EC} \tag{12}$$

where

$$g_o = \frac{df}{d\,E^2_{MAX}}\ \frac{2\,V_{EB}}{d^2} \tag{13}$$

$$\mu_o = \frac{q\,N_D}{K}\ \frac{d^2}{V_{EB}} \tag{14}$$

i_g = the small signal generator current

v_{EB} = the small signal emitter base voltage

v_{EC} = the small signal emitter collector voltage

The equivalent circuit which describes this behavior is given in Figure 2. Here r_{EB} is the resistance of the insulator between the two metals. (The resistance associated with the two reverse biased diodes has been neglected here.) From Figure 2 we see that

$$v_{EB} = r_{EB}\, i_B \tag{15}$$

$$i_c = g_o\, r_{EB}\, i_B - g_o\, \mu_o\, v_{EC} \quad . \tag{16}$$

Therefore, the collector current becomes

$$i_c = \beta\, i_B - g_o \mu_o\, v_{EC} \tag{17}$$

where

β = short circuit common emitter current gain.

The maximum available matched power gain is thus

$$PG = \frac{g_o\, r_{EB}}{4\, \mu_o} = \frac{\beta}{4\, \mu_o} \quad . \tag{18}$$

μ_o may be calculated from a previous equation. For 1 ohm-cm, n-type germanium, V_{EB} is one volt, d is 50 Å, and $\mu_o \approx 5 \times 10^{-5}$. Thus, high power gains are available even with modest values of β.

This analysis has been extended to the case where the reverse biased diode impedances r_{EC} and r_{BC} are included, and to the case where series resistances r'_E and r'_B are included in the emitter and base arms, respectively. These analyses shows that r_{EC} serves only to degrade the output impedance, r'_B serves only to increase the input impedance, while r_{BC} and r'_E each affect all four of the common emitter hybrid parameters. In practice, however, the most important variable has been found to be the parasitic resistance r_{EB} between the two metal layers. Since r_{EB} and β are directly related, any tendency for the two metals to short-out destroys the unit. Therefore, achieving thin compact insulating layers to act as very thin spacers between the two metals is the most important problem in the fabrication of MEA structures.

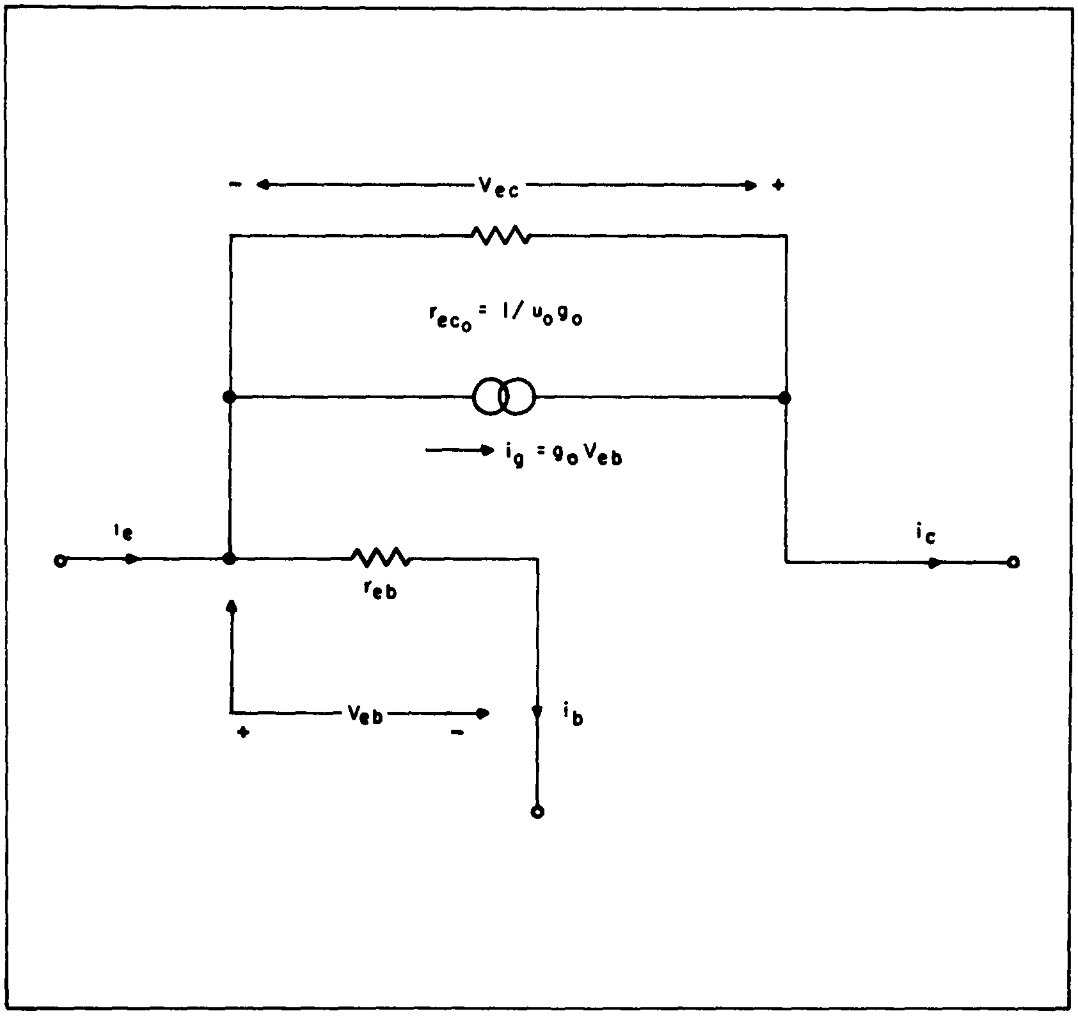

FIGURE 2 EQUIVALENT CIRCUIT OF MEA DEVICE (NEGLECTING IMPEDANCES OF REVERSE BIASED DIODES)

a. Characteristics of MEA Devices

Fabrication of MEA devices of the type discussed above is severly hampered by shorting between the two metal electrodes. This results in a very low yield of usable devices. However, those units which can be studied exhibit rather good characteristics. Measurements have been made of the three-terminal DC "h" parameters, the temperature dependence of the input I-V characteristics and the current gain, α, and the frequency response. These measurements are discussed below.

(1) DC "h" Parameters

Figures 3 (a) and (b) shows typical common base output and transfer curves for MEA devices in the two modes of operation, normal and reverse. The normal mode is that in which the first film to be deposited is used as the base of the device, and the reverse mode is that in which the first film to be deposited is used as the emitter. In the simplified model discussed above, the characteristics obtained in these two modes would be expected to be identical. Deviation in geometry from the ideal would, however, be expected to favor one mode over the other, so that the differences seen between Figures 3(a) and (b) are not surprising.

Measurements have been made of the common base characteristics of these devices as a function of temperature. The parameters measured have been the input I-V curves and the collector current versus emitter current. Figure 4 shows I_E vs V_{EB} at 22°C. This curve shows that the total emitter current is the sum of that flowing through a constant conductance G_s, and an exponentially varying component. Similar separations have been made at +10°C, -10°C, -50°C, -100°C, and -195°C. The constant conductance G_s could be obtained at each temperature, the exponential term determined, and the dependence of collector current on the exponential emitter current also obtained. These data are shown in Figures 5, 6, and 7. These results show rather conclusively that the input I-V characteristic is the sum of a high resistance short term I_G, and a tunneling-like characteristic I_B. The former term is not contributing to I_c, the gain of the device being determined by the ratio of I_B to I_G. Furthermore, the current gain $\Delta I_c/\Delta I_B$ is independent of temperature. All of these characteristics are in agreement with that expected from the MEA model.

(2) Frequency Characteristics

Some AC data have been obtained on MEA devices, indicating that the gain mechanism is fast, provided parasitic terms can be minimized. Power gain of 10 db at 10 mc has been measured, and devices have been made to oscillate at frequencies as high as 42 mc. If the shorting problem described below could be minimized, a useful device could be obtained which might offer substantial improvements in radiation resistance over conventional bipolar devices.

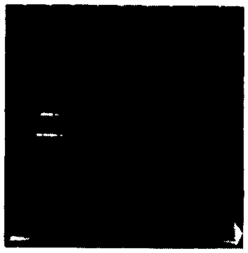

I_C = 1ma/DIV

V_{CB} = 0.5V/DIV

ΔI_E = 1ma/STEP

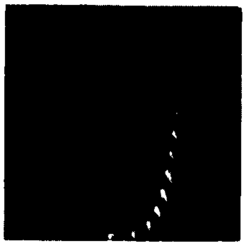

I_C = 1ma/DIV

V_{EB} = 0.5/DIV

ΔI_E = 1ma/STEP

NORMAL

AT $V_{CB} = 2.5V$, $I_E = 6ma$

h_{11} = 50 ohms

h_{12} = 0.02

h_{21} = −0.8

$h_{22} = 10^{-4}$ mhos

P.G. = 10

FIGURE 3a COMMON BASE CHARACTERISTICS OF EDGE DEVICE IN NORMAL DIRECTION

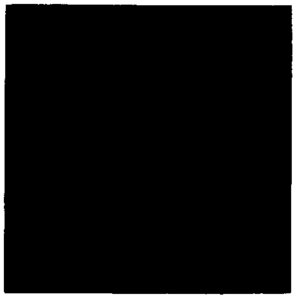

I_C = 0.5ma/DIV

V_{CB} = 0.5V/DIV

ΔI_E = 0.5ma/STEP

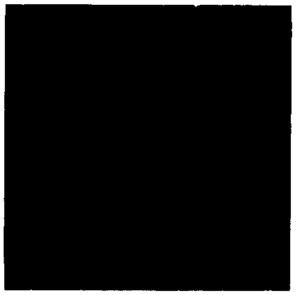

I_C = 0.5V/DIV

V_{EB} = 0.5V/DIV

ΔI_E = 0.5ma/STEP

REVERSE

AT $V_{CB} = 2.5V$, $I_E = 6ma$

h_{11} = 100 ohms

$h_{12} \approx 0$

h_{21} = −0.8

$h_{22} < 1.7 \times 10^{-5}$

P.G. > 100

FIGURE 3b COMMON BASE CHARACTERISTICS OF EDGE DEVICE IN REVERSE DIRECTION

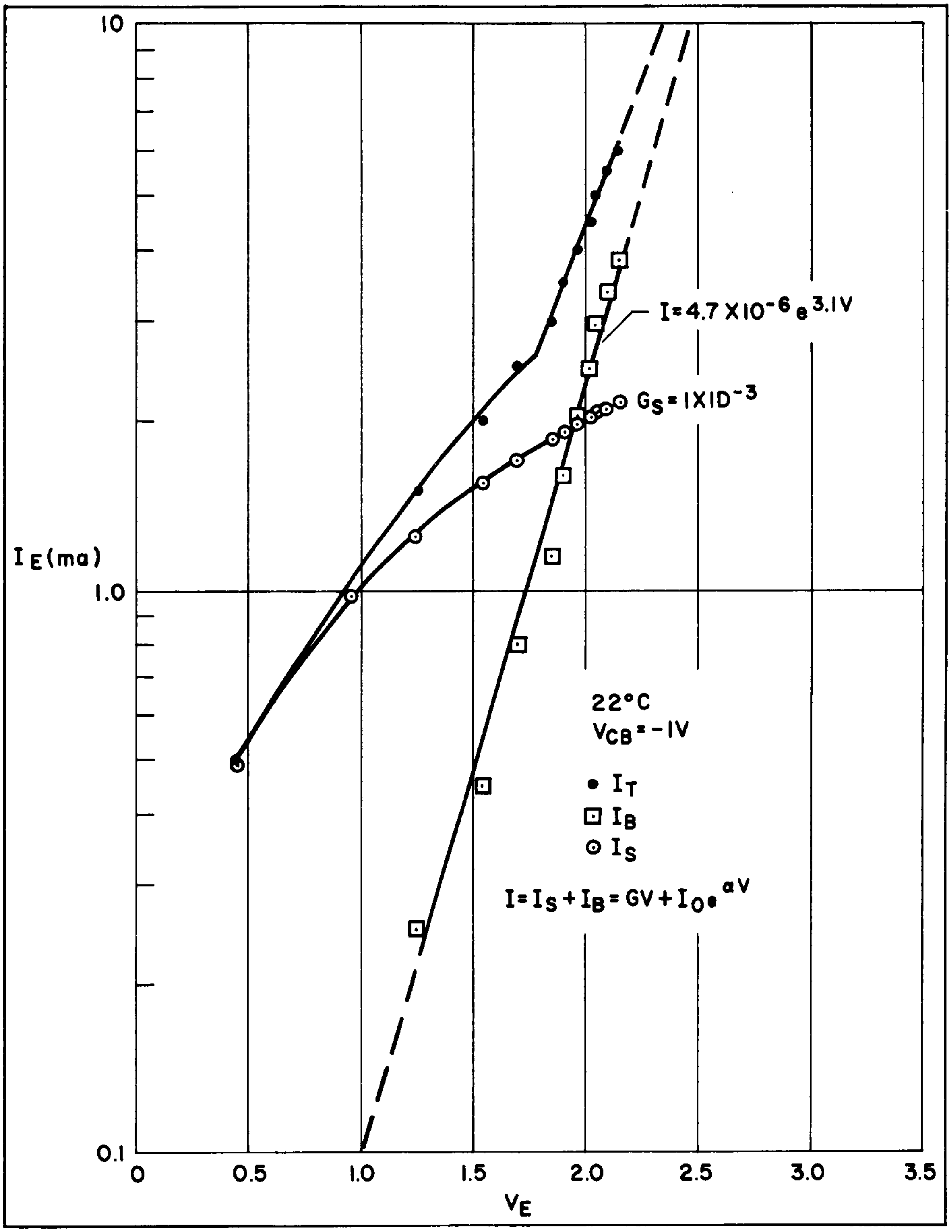

FIGURE 4 I_E-V_{EB} FOR MEA (REVERSE)

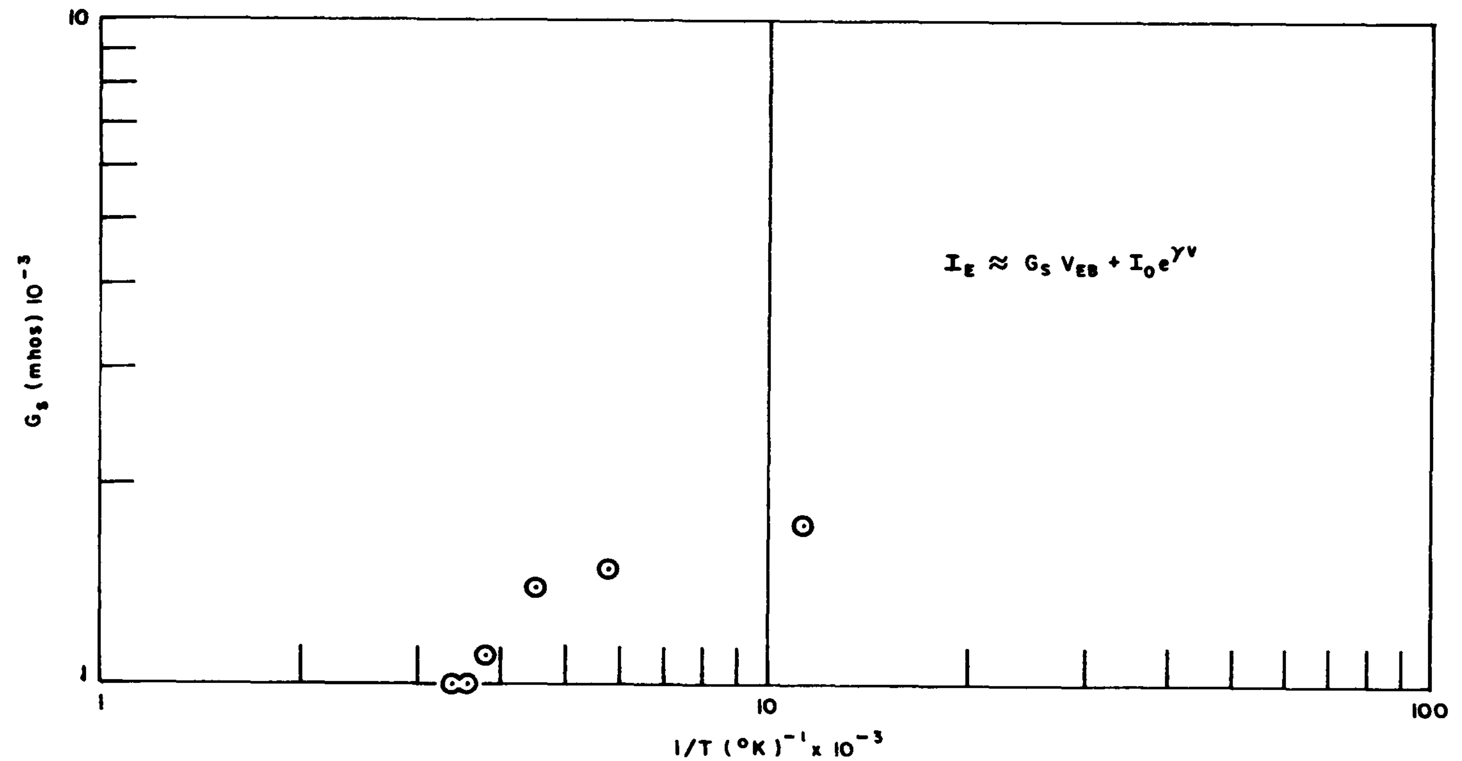

FIGURE 5 G_S VERSUS T

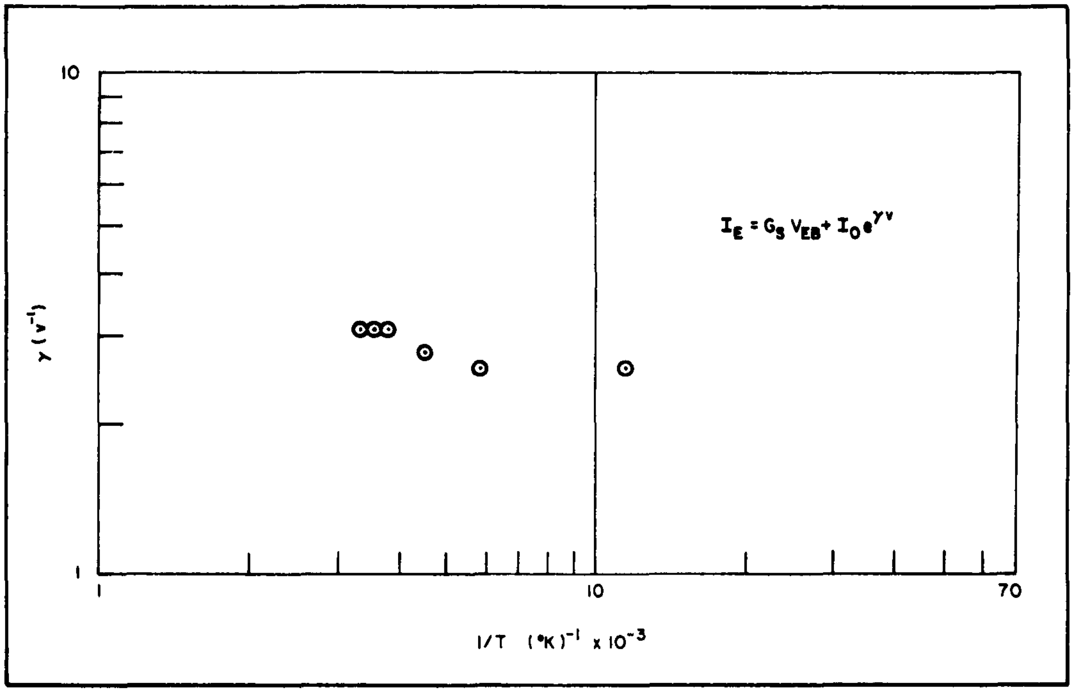

FIGURE 6a γ VERSUS 1/T

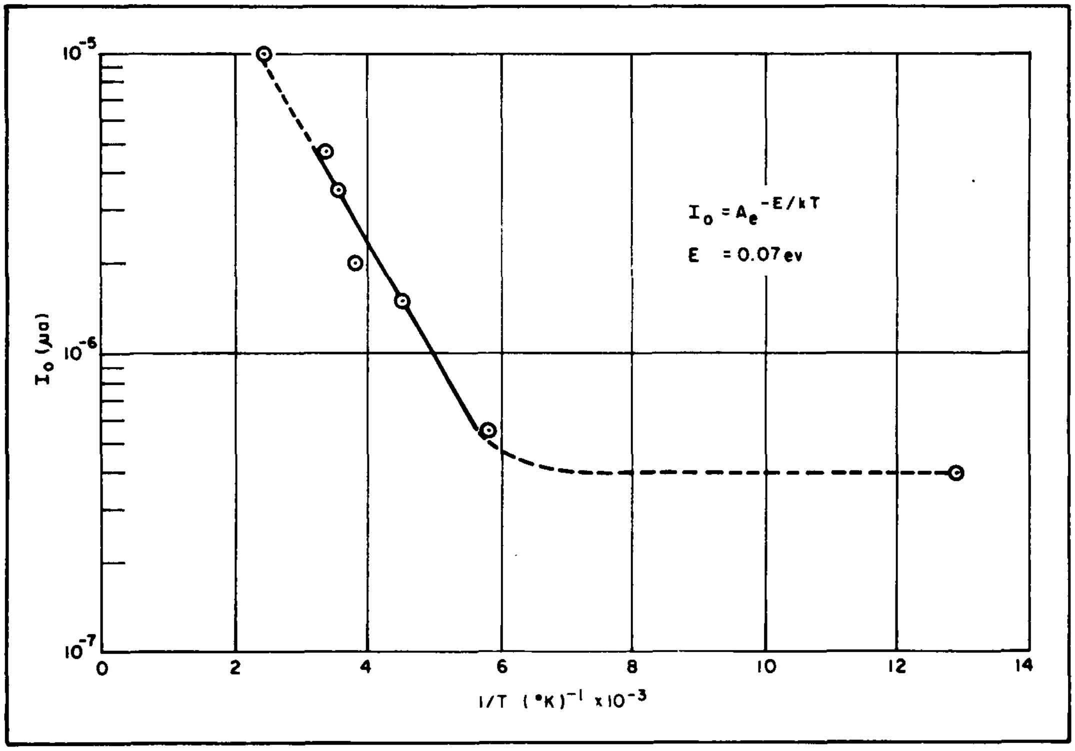

FIGURE 6b I_0 VERSUS 1/T

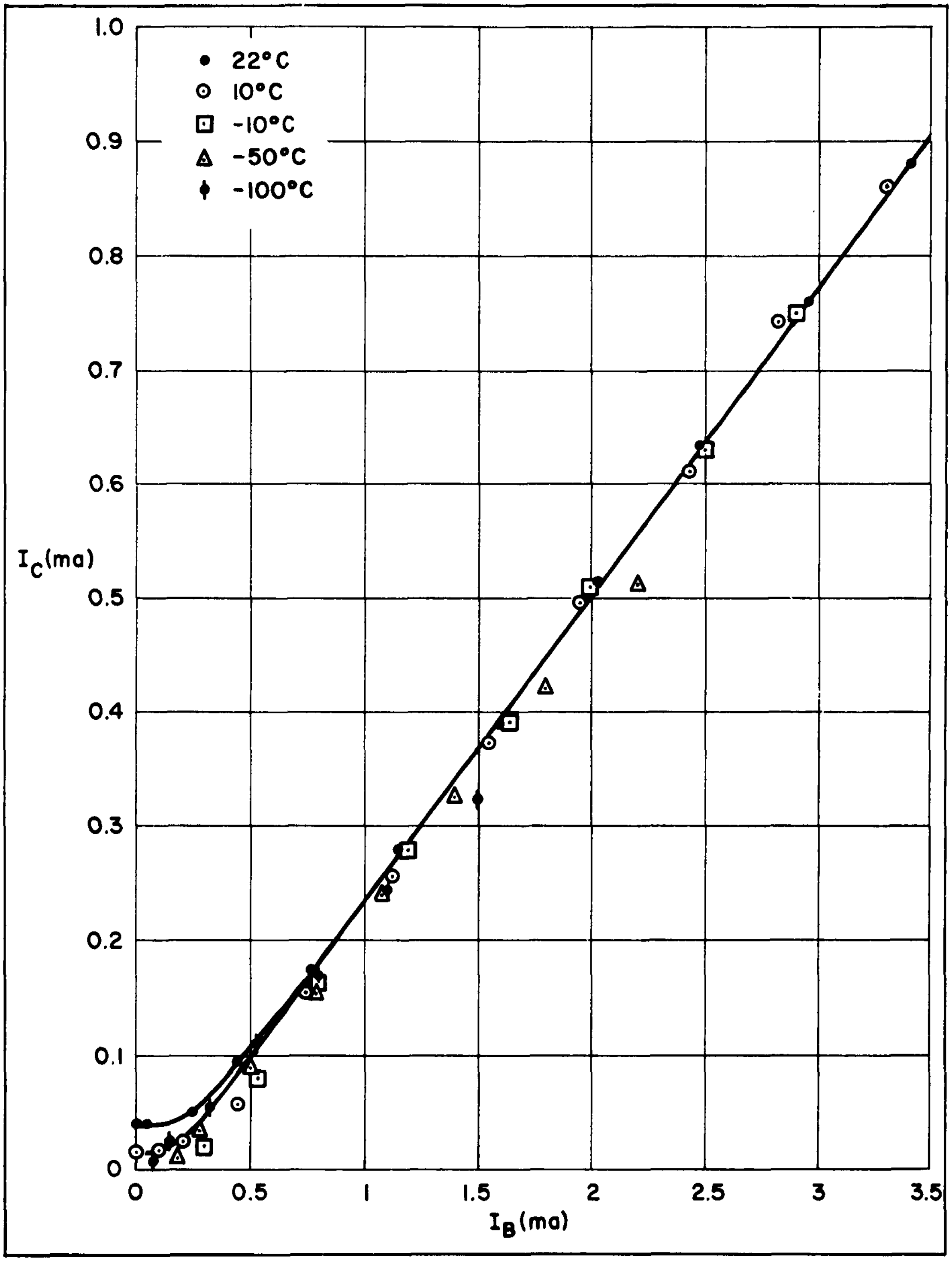

FIGURE 7 I_C VERSUS I_B VERSUS TEMPERATURE (SLOPE IS α)

B. Theoretical Analysis

The main areas of theoretical interest in the field of hot electron devices are those of injection, transport, and collection. The first two of these have been treated in sufficient detail[4, 5, 10] to outline the general device design criteria for emitters and bases. The third, however, has received little attention other than a few comments by Hall.[15] Therefore, an analysis was made of the factors affecting collection of hot electrons once injected and transported. Three mechanisms are found to affect the collection efficiency (and through it the current gain); viz., quantum reflections at a potential barrier, critical angle for collection at the interface between regions of different carrier velocities, and backscattering out of the collector material. These three mechanisms are analyzed below.

1. Quantum Reflections at a Potential Barrier

If an electron arrives at a potential barrier at normal incidence, there is, according to quantum mechanics, a certain probability that it will be reflected due to the wave nature of the electron. The amount of this reflection can only be calculated if the detailed shape of the barrier is known. This effect should not be very important unless the potential changes rapidly within several angstroms (which it may). In any event, it should be of less importance as the energy increases above the barrier height ϕ_o (see Figure 8).

An upper limit on the amount of losses which can occur from this effect can be calculated by assuming that the potential changes abruptly at the barrier and all carriers are incident normally on the barrier. Then, the fraction of the electrons collected f_c will be, using results of Bohm, "Quantum Theory," Prentice-Hall, 1952, p. 229.

$$f_c = \frac{4\left[E_M E_S\right]^{1/2}}{\left(E_M^{1/2} + E_S^{1/2}\right)^2} \tag{19}$$

where

E_M = the kinetic energy of the electron in the metal

E_S = the kinetic energy of the electron in the semiconductor.

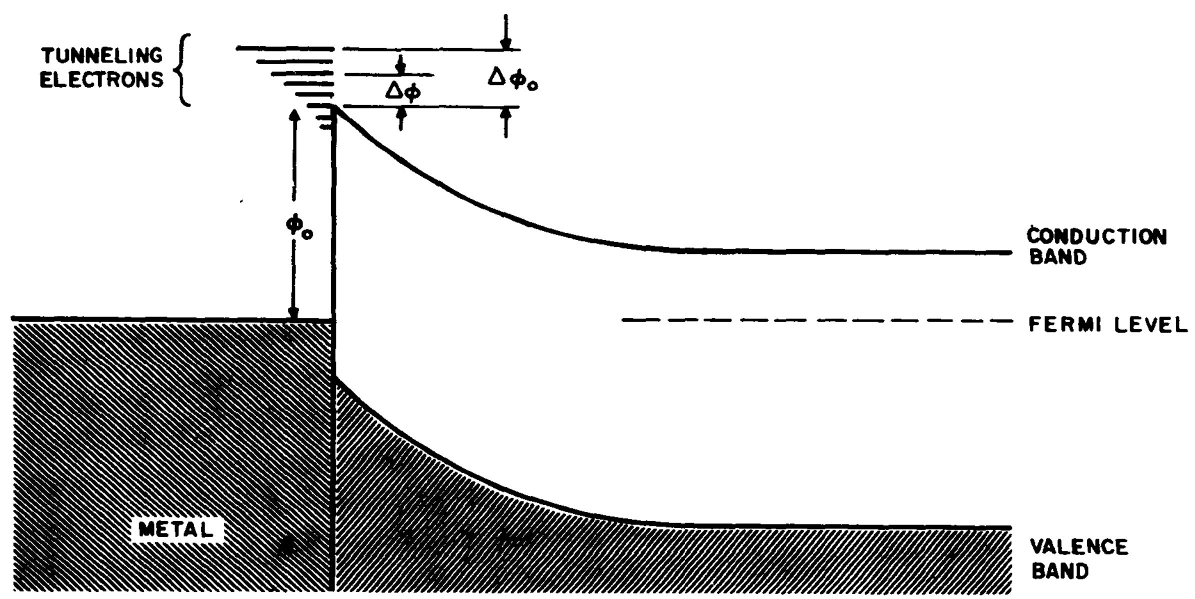

FIGURE 8 ENERGY DIAGRAM OF METAL - SEMICONDUCTOR INTERFACE

If $E_M = 5$ ev, then for

$$E_S = 0.05 \text{ ev}, \quad f_c \geq 0.33$$

$$E_S = 0.5 \text{ ev}, \quad f_c \geq 0.73$$

2. Critical Angle for Collection at an Interface

There is a critical angle, θ_c, within which an electron in the metal having energy sufficient to cross the surface barrier must strike the barrier in order to conserve lateral momentum in the process. This angle is given by[3]

$$\sin^2 \theta_c = \left(\frac{E_M - E_F - q\,\phi_o}{E_M}\right) \left(\frac{m_s^*}{m_m^*}\right) \qquad (20)$$

where

E_M = electron kinetic energy in the metal

E_F = Fermi energy in the metal

ϕ_o = barrier height between metal and semiconductor

m_m^*, m_s^* = effective electron mass in metal and semiconductor, respectively.

Thus, if an electron arrives 0.05 ev above the barrier with a kinetic energy of 5 ev, it must strike within 6^o of the normal to be collected, whereas an electron 0.5 ev above the barrier must strike within 18^o of the normal to be collected. Therefore, unless the hot electrons strike the barrier with energies substantially greater than the barrier height, they must be well directed normally to be collected.

a. Angular Distribution of Electron Velocities in Tunnel Emission of Hot Electrons

In order to determine the seriousness of the critical angle requirements for collection, we must consider the distribution in angle of tunnel emitted electrons. It can be shown that the distribution in angle and energy of tunnel injected hot electrons is [3]

$$\frac{d_j(\Delta\phi, \theta)}{j_{total}} \approx \frac{e^{-\left\{\frac{\Delta\phi_o - \Delta\phi}{\overline{W}}\right\}} \; e^{-\frac{\sin^2\theta}{\sin^2\alpha}} \, d(\Delta\phi)d(\sin^2\theta)}{\overline{W}\sin^2\alpha} \quad (21)$$

where

$\Delta\phi_o$ = the energy above the barrier height of the most energetic of the tunneling electrons (cf. Figure 8)

$\Delta\phi$ = the energy of any particular tunneling electron above the barrier height

θ = the angle of incidence of hot electrons on both emitter and collector sides of base (emitter and collector assumed parallel)

$\overline{W}$ = the mean spread in energy of tunneling electrons

α = the mean angular spread in tunneling electrons

Furthermore,

$$\sin^2\alpha = \frac{\overline{W}}{E_F + \phi_o + \Delta\phi} \quad (22)$$

and

$$\sin^2\theta_c = \frac{\Delta\phi}{E_F + \phi_o + \Delta_\phi} \quad (23)$$

where

E_F = Fermi energy in the metal

ϕ_o = barrier height.

Integrating $d_j(\Delta\phi, \theta)/j$ between $\theta = 0$ and $\theta = \theta_c$, we find for the fraction of the electrons which will enter the collector between $\Delta\phi$ and $\Delta\phi + d(\Delta\phi)$

$$\frac{d_j(\Delta\phi)}{j_{total}} \approx e^{\frac{-\Delta\phi_o - \Delta\phi}{\overline{W}}} \left(1 - e^{\frac{\Delta\phi}{\overline{W}}}\right) \frac{d\Delta\phi}{\overline{W}} \quad . \tag{24}$$

Then the total fraction f of the electrons injected which can enter the collector is obtained by integrating over $\Delta\phi$ from 0 to $\Delta\phi_o$

$$f = \frac{j_{collected}}{j_{injected}} \approx 1 - \left(\frac{\Delta\phi_o}{\overline{W}} + 1\right) e^{\frac{-\Delta\phi_o}{\overline{W}}} \quad . \tag{25}$$

Table I lists values of f for various values of $\Delta\phi_o/\overline{W}$ and shows that for high collection efficiencies, $\Delta\phi_o$ must be several times $\overline{W}$.

TABLE I

TOTAL FRACTION OF INJECTED ELECTRONS COLLECTABLE

$\Delta\phi_o/\overline{W}$	1	2	3	4	5
f	0.26	0.57	0.8	0.91	0.96

The quantity $\overline{W}$, the mean spread in energy of the tunneling electrons, must be greater than kT, since $1/\overline{W}$ measures the rate at which the tunneling probability changes with the energy of the incident electron. If $\overline{W}$ were less than kT, the Fermi-Dirac distribution function in the emitter would be decreasing less rapidly with increasing electron energy than the tunneling probability increases, so that the electrons in the emitter would be more likely to go over the top of the barrier than tunnel through it. Therefore, to achieve high collection efficiencies, $\Delta\phi_o$ must be at least several times kT for a tunnel input device.

3. Backscattering out of the Collector

If an electron has the proper values of energy and momentum to pass into the conduction band of the collector, it can still fail to be collected if a collison in the collector barrier material causes it to be scattered back into the base film. This can occur if a large momentum loss collision occurs before the electron loses enough energy to be prevented by the collector field from passing back into the base. If the electron enters the collector barrier with an energy in the range between the optical phonon energy and the gap width E_g, optical phonon collisions could provide such a process. Optical phonon energies for various materials are listed in Table II, and can be seen generally to run not much greater than 0.10 ev.

TABLE II

OPTICAL PHONON ENERGIES
FOR VARIOUS MATERIALS

Material	Optical Phonon Energy
InSb	0.023[16]
GaSb	0.029[17]
InAs	0.029[17]
GaAs	0.035[17]
Ge	0.037[17]
InP	0.042[17]
SiC	0.010

Thus, if an electron enters the collector with an excess energy of 1.0 ev, it must be scattered approximately 10 times before it has lost sufficient energy to be assured of being collected. If, as a result of one or more of these scatterings the electron returns into the base metal, it will be difficult for it to be rescattered into the critical angle in order to again enter the collector, and will thus, to a good approximation, be lost for collection. The complete solution of the effect of backscatterings on the collection efficiency of a hot electron triode requires a knowledge of:

(i) The distribution in momentum and energy of electrons scattered by optical phonons in the presence of an applied field,

(ii) the effect of quantum reflections at the base collector interface on the transmission of this interface to both incident and scattered electrons, and

(iii) the probability of electrons being rescattered into the collector after being rejected once by the collector.

Such a solution would be extremely difficult, but the general features of backscattering can be illustrated by considering the following question: "If an electron enters a collector material (in which it is assumed that no field exists) at an arbitrary angle, and has a certain mean free path after which it is scattered losslessly at an arbitrary angle, what is the probability that after n collisions it will recross the surface where it entered (neglecting quantum reflections) and thus return to the base?" This problem has been treated by A. Berman of Philco Scientific Laboratory, and the results are shown in Table III.

TABLE III

PROBABILITY OF ELECTRON RETURNING TO BASE

Number of Scatterings	Fraction of Electrons Lost	Fraction of Electrons not Lost
1	0.25	0.75
2	0.125	0.625
3	0.078	0.547

Although the general solution could not be obtained, Table III indicates that the achievement of high collection efficiencies will be unlikely unless special collection barrier designs are employed. The approach which led to these results is discussed below.

a. Probability of Hot Electron Backscattering

(1) Single Collision

Assume that electrons enter material 2 in Figure 9(a) (which material is semi-infinite) at $x = 0$ with a momentum of magnitude $/p/$ and direction θ_1 distributed uniformly between $\theta_1 = 0$ and $\theta_1 = \pi/2$. If, after traveling a distance r these electrons undergo lossless collisions into an angle θ_o (where θ_o is randomly distributed between $\theta_o = 0$ and $\theta_o = \pi$), all those carriers for which θ_o is between 0 and $\pi/2$, and which suffer no further collisions before traveling a distance $r \cos \theta_1 \sec \theta_o$, will pass back into the material. Thus if α_1 is the fraction backscattered into the base after one collision

$$\alpha_1 = \frac{1}{2} \int_o^{\pi/2} d\theta_1 \int_o^{\pi/2} d\theta_o \int_o^{\infty} \sin \theta_1 \sin \theta_o \; e^{-\frac{r}{\lambda}\left(1 + \frac{\cos \theta_1}{\cos \theta_o}\right)} dr \tag{26}$$

where

$\sin \theta_1 \, d\theta_1$ = the fraction of initial electrons entering region 2 between θ_1 and $\theta_1 + d\theta_1$

$e^{-r/\lambda} \frac{dr}{\lambda}$ = the fraction undergoing a collision between r/λ and $(r + dr)/\lambda$

$\frac{1}{2} \sin \theta_o \, d\theta_o$ = the fraction scattered into an angle between $\theta_o + d\theta_o$

$e^{-\frac{r \cos \theta_1}{\lambda \cos \theta_o}}$ = the fraction traveling back to the interface without collision.

If the above integration is carried out, we see that

$$\alpha_1 = \frac{1}{4} \quad . \tag{27}$$

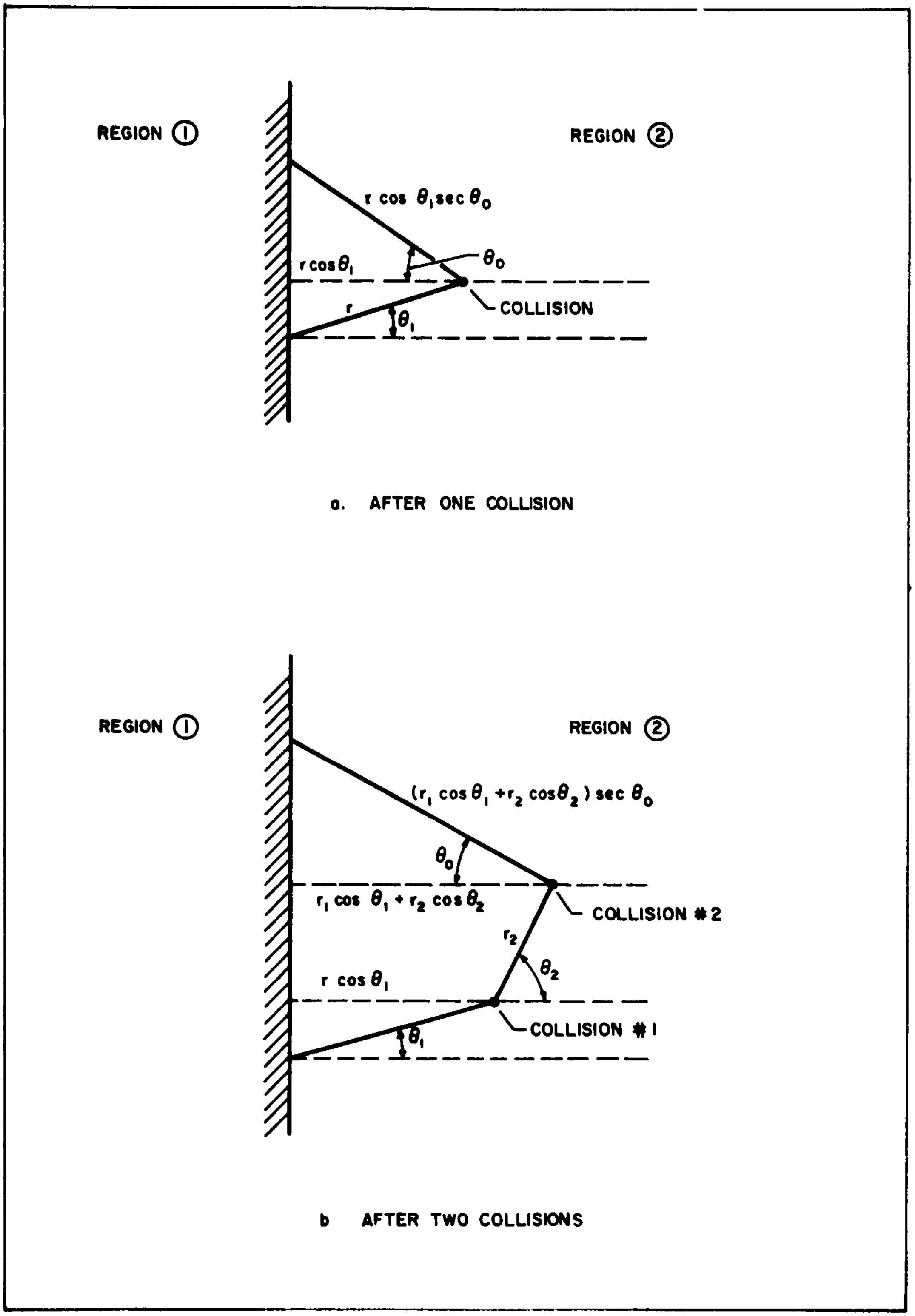

FIGURE 9 BACKSCATTERING

(2) Two Collisions

To determine the number backscattered by two collisions we see that:

(i)	$\sin\theta_1\, d\theta_1$ = the fraction of the incident electrons entering region 2 between θ_1 and $\theta_1 + d\theta_1$, where θ_1 is between 0 and $\pi/2$ (cf. Figure 9b).
(ii)	$e^{-\frac{r_1}{\lambda}}\, d(\frac{r_1}{\lambda})$ = the fraction undergoing a collision between $\frac{r_1}{\lambda}$ and $\frac{r_1 + dr_1}{\lambda}$, where $\frac{r_1}{\lambda}$ varies between zero and infinity.
(iii)	$1/2 \sin\theta_2\, d\theta_2$ = the fraction scattered into an angle between θ_2 and $\theta_2 + d\theta_2$, where θ_2 varies between zero and π.
(iv)	$e^{-\frac{r_2}{\lambda}}\, d(\frac{r_2}{\lambda})$ = the fraction undergoing a collision between $\frac{r_2}{\lambda}$ and $\frac{r_2 + dr_2}{\lambda}$, where $\frac{r_2}{\lambda}$ varies between zero and infinity for θ_2 between 0 and $\pi/2$, and between zero and $-\frac{r_2}{\lambda}\frac{\cos\theta_1}{\cos\theta_2}$ for θ_2 between $\pi/2$ and π.
(v)	$1/2 \sin\theta_o\, d\theta_o$ = the fraction scattered into an angle between θ_o and $\theta_o + d\theta_o$, where θ_o varies between zero and $\pi/2$.
(vi)	$e^{-\frac{1}{\lambda}(r_1 \cos\theta_1 + r_2\cos\theta_2)\sec\theta_o}$ = the fraction passing back into region 1 after the second collision without any further collisions.

Thus, if a_2 is the fraction backscattered into the base after two collisions, and if we let $x_i = r_i/\lambda$, and $u_i = \cos\theta_i$, then

$$a_2 = \frac{1}{4}\int_o^1 du_o \int_o^1 du_1 \int_o^\infty dx_1 \left\{ \int_o^1 du_2 \int_o^\infty dx_2 + \int_{-1}^o du_2 \int_o^{\frac{-x_1 \mu_1}{\mu_2}} dx_2 \right\}$$

$$e^{-x_1\left(1 + \frac{\mu_i}{\mu_o}\right) \; -x_2\left(1 + \frac{\mu_2}{\mu_o}\right.} \quad . \tag{28}$$

Integration of this expression shows that

$$a_2 = \frac{1}{8} \quad . \tag{29}$$

(3) n Collisions

The above analysis can be extended to the case of n collisions, and an integral set up for this case. Unfortunately, the integration cannot be performed for the general case. If it is felt, however, that values of a_n for $n > 3$ would be informative, attempts at machine calculation could be made. The general result, using the above notation, is

$$a_n = \frac{1}{2^n}\int_o^1 du_o \int_o^1 du_1 \int_o^\infty dx_1 \; e^{-x_1\left(1 + \frac{\mu_i}{\mu_o}\right)} \prod_{k=2}^{n} \left\{ \int_o^1 du_k \int_o^\infty dx_k \right.$$

$$\left. + \int_{-1}^o du_k \int_o^{-\sum_{i=1}^{k} u_i x_i / u_k} dx_k \right\} \quad e^{-x_k\left(1 + \frac{u_k}{u_o}\right)} \quad . \tag{30}$$

C. Experimental Results - MEA Device

The considerable effort expended by Philco on the MEA device prior to the start of this program (cf. Section IV-A-2) has shown the basic feasibility of this approach to a tunneling device and indicated potential applicability to thin film structures. Serious fabrication problems had been encountered however; viz., a tendency for the emitter and base films to short. The data in Figure 4, showing an ohmic conductance G_s in parallel with the emitter barrier led us to believe that the shorting occurred through the thermally grown Al_2O_3 layer rather than along the hole-rich surface of the germanium (produced by the surface barrier contacts) because of the positive temperature coefficient observed for G_s. Therefore, extensive studies of oxidation techniques were conducted in an attempt to eliminate what were felt to be weak spots or pinholes in the Al_2O_3 layer. No technique has been discovered which improves the shorting problem. In fact, this problem seems to be getting worse. Therefore, a fundamental study of the thermal oxidation of aluminum has begun, and until more information on the details of the oxidation process are available, evaporated insulators will be studied for device fabrication purposes. The unsuccessful steps taken in the device program to eliminate emitter-base shorts and their justification are discussed below, and the results of a large number of device runs are shown.

1. Thermal Oxidation of Aluminum

The fabrication technique presently being used for fabrication of MEA devices involves chemically etched (10 parts HNO_3, 3 parts HF, 3 parts acetic acid) n-type germanium of < 110 > orientation. Sixty-mil cubes of this material are soldered on TO-5 stems, using gold-0.5% phosphorus solder. A platen holding sixteen such stems is placed in the vacuum system, and a phosphor bronze mask with 0.010" x 0.015" slots is positioned 0.005" above the surface of the germanium. Two pre-fired tungsten coils containing 99.99% pure Al (Cominco 99.9999% pure Al has also been used) are positioned above the platen-mask assembly, the first 4.5" directly above, the second 4.5" above and 5" to the left. The vacuum system is then pumped out, and aluminum evaporated at an angle from the second filament. The resultant film is then oxidized, the system again pumped out, and the second film evaporated from the other tungsten filament. Because of the angle of the first evaporation, the two films are partially overlapped, and the entire process can be performed without exposing the device to ambient. Gold wire 0.002" in diameter is then thermocompression bonded to each of the aluminum films, and the unit is canned in nitrogen containing less than 5 ppm water vapor. This process seems adequate with the exception of the oxidation of the first aluminum film.

The standard oxidation technique used in devices employing Al_2O_3 has been a 1 hour, 22°C oxidation in air dried by passing it through a dry ice-methanol trap and molecular sieve. According to the results of Hunter and Fowle,[18] such a process should produce a compact, amorphous, barrier-type oxide about 10 Å thick. Furthermore, such oxides have in the past produced usable emitter barriers. The low yield of this process, however, has led us to attempt oxidations at higher temperatures which should produce thicker oxides.[18] If the shorting was due to weak spots or pinholes in the oxide formed at 22°C, a higher temperature oxide should decrease the number of shorts. This, however, was not found to be the case. Table IV shows the results of higher temperature oxidation studies.

TABLE IV

HIGHER TEMPERATURE OXIDATION OF ALUMINUM

Run #	Oxidation Temperature (°C)	Oxidation Time (hrs)	Characteristics of Emitters (4 units each run)
60	100	1	largely shorts
61	150	1.5	largely shorts
62	150	2	largely shorts
63	225	1	largely shorts
64	225	2	all shorts
65	150	2	all shorts
66	150	2	all shorts
69	120	2	all shorts

In addition to oxidizing at higher temperatures, exposing the aluminum-air interface to ultraviolet illumination was also attempted to increase the oxide film thickness. It has been reported[19, 20, 21] that the self-limiting thickness of Al_2O_3 on aluminum is increased by such exposure. Therefore, four groups of 16 triode structures each were oxidized at 22°C in the standard fashion except that they were illuminated by light from an Osram mercury lamp (Hg S) (50 candles luminous intensity) placed 6 inches from the films. Table V shows conditions of these four runs and the results.

TABLE V

EFFECT OF UV ILLUMINATION
ON ALUMINUM OXIDE THICKNESS

Run #	Oxidation Time (hrs)	Characteristics of Emitters
111	1	Shorts
112	2	Open
113	1	Shorts
114	1.5	Shorts

Recent work by C. Kirk at Lincoln Laboratory on the oxidation of aluminum[22] has indicated that the surface states associated with the chemisorption of oxygen at the metal oxide-oxygen interface controls the oxidation of aluminum. In that case, the vacuum level at which the aluminum film (to be oxidized) is deposited might affect the quality of the resultant oxide film. To check this point, triodes were fabricated in which the aluminum was deposited in pressures varying from 10^{-9} to 10^{-5} torr. Again, no consistent effect on emitter-base shorting was observed, as seen in Table VI. Oxidation temperature for each run was 22°C.

TABLE VI

EFFECT OF VARIOUS PRESSURES
ON ALUMINUM OXIDE QUALITY

Run #	Evaporation Pressure	Oxidation Time (hrs)	Characteristics of Emitters
131	3.5×10^{-9}	2	Shorts
129	2×10^{-8}	1	Shorts
128	2×10^{-6}	4	Shorts
117	2×10^{-5}	1	Shorts

2. Aluminum Films

The other variables studied in an attempt to eliminate emitter-base shorts have been those affecting the quality of the aluminum films; viz., resistivity, thickness, structure of the films, substrate flatness, and overlap of the films. Again, no dependence of shorts on any of these parameters has been seen.

The resistivity of the aluminum films used in MEA devices has been found to very as expected with deposition rate. Figure 10 shows results obtained using a deposition rate between 500 and 1000 Å/sec. Slower deposition rates have produced higher values of ρ for a given t, but the difficulty in measuring rate prevents quantitative analysis.

Both the first and second films evaporated have been varied in thickness over the range from 100 to 2000 Å, and little effect on triode parameters seen. In general, more good units are obtained when the films are thin, but this could be due only to the fact that more thin units are made.

The amount by which the two films overlap can be varied by varying the spacing between the mask and the substrates. Since the long sides (0.015") of the films are overlapped, and since contact must be made

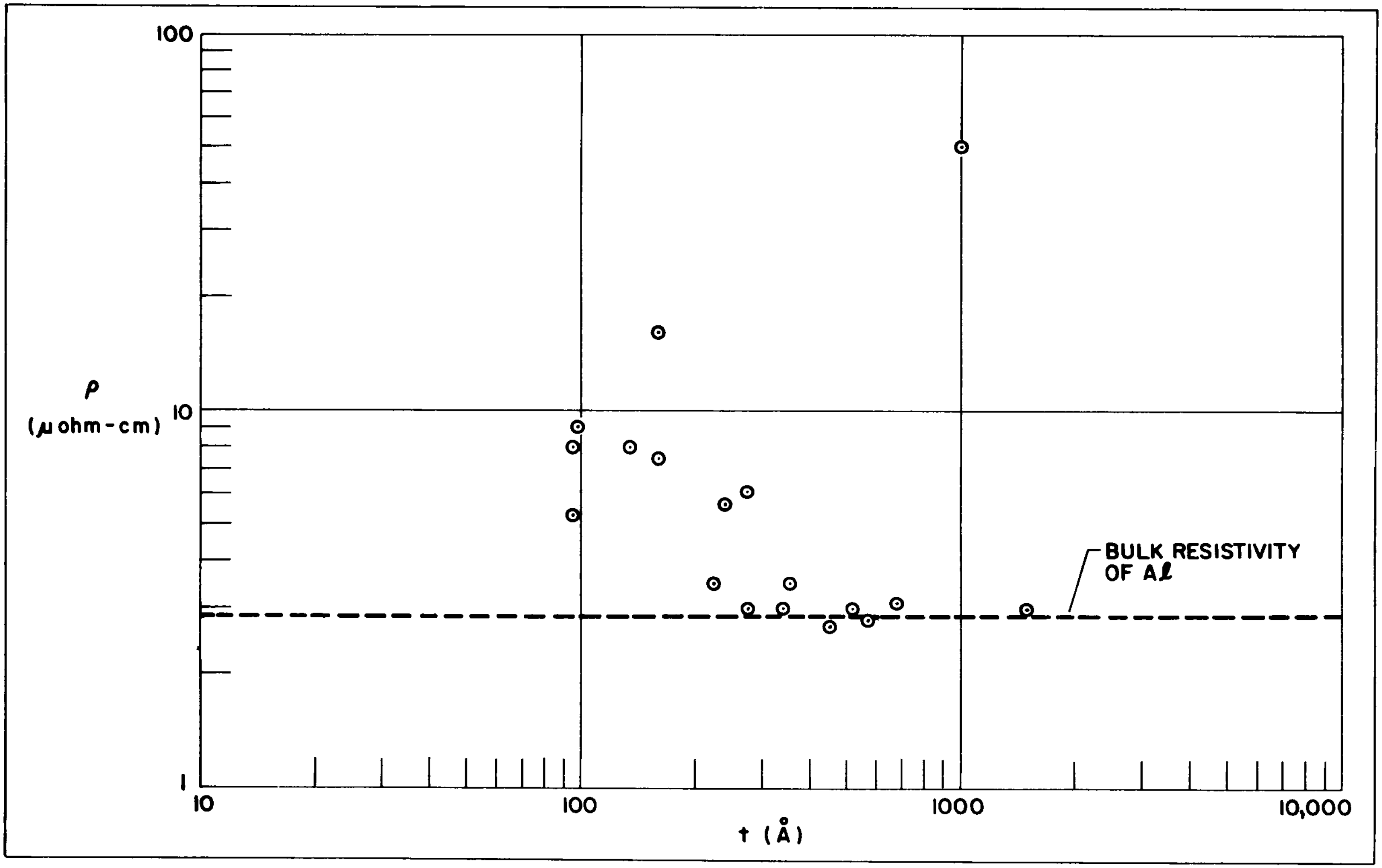

FIGURE 10 RESISTIVITY OF ALUMINUM FILMS VERSUS THICKNESS

to each film separately, overlap dimensions are limited to the range from 0.001" to 0.009". This range has been covered with no apparent effect on shorting.

The structure of evaporated aluminum films and the flatness of the substrates used are also under study. Little data are available on structure, but replicas of chemically etched germanium surfaces show exceptionally good local flatness. Figure 11 is an electron micrograph of a surface shadowed with Au-Pd, stripped, and viewed in transmission. The magnification is 80,000 X. The only texture visible, with the exception of isolated particles of "dust" is that of the shadowing material. Continued studies may give pertinent information on the aluminum films themselves.

In addition to germanium surfaces, GaAs and glass have also been used to study emitter-base shorts. Neither produced consistent results. Because of the severity of this shorting problem, it is felt that an inert substrate, e.g., glass, should be used for continued study of the natural oxide of $A\ell$, and triode work restricted to use of evaporated oxides. Preliminary work on this approach is currently being done and will be reported in the next quarterly report.

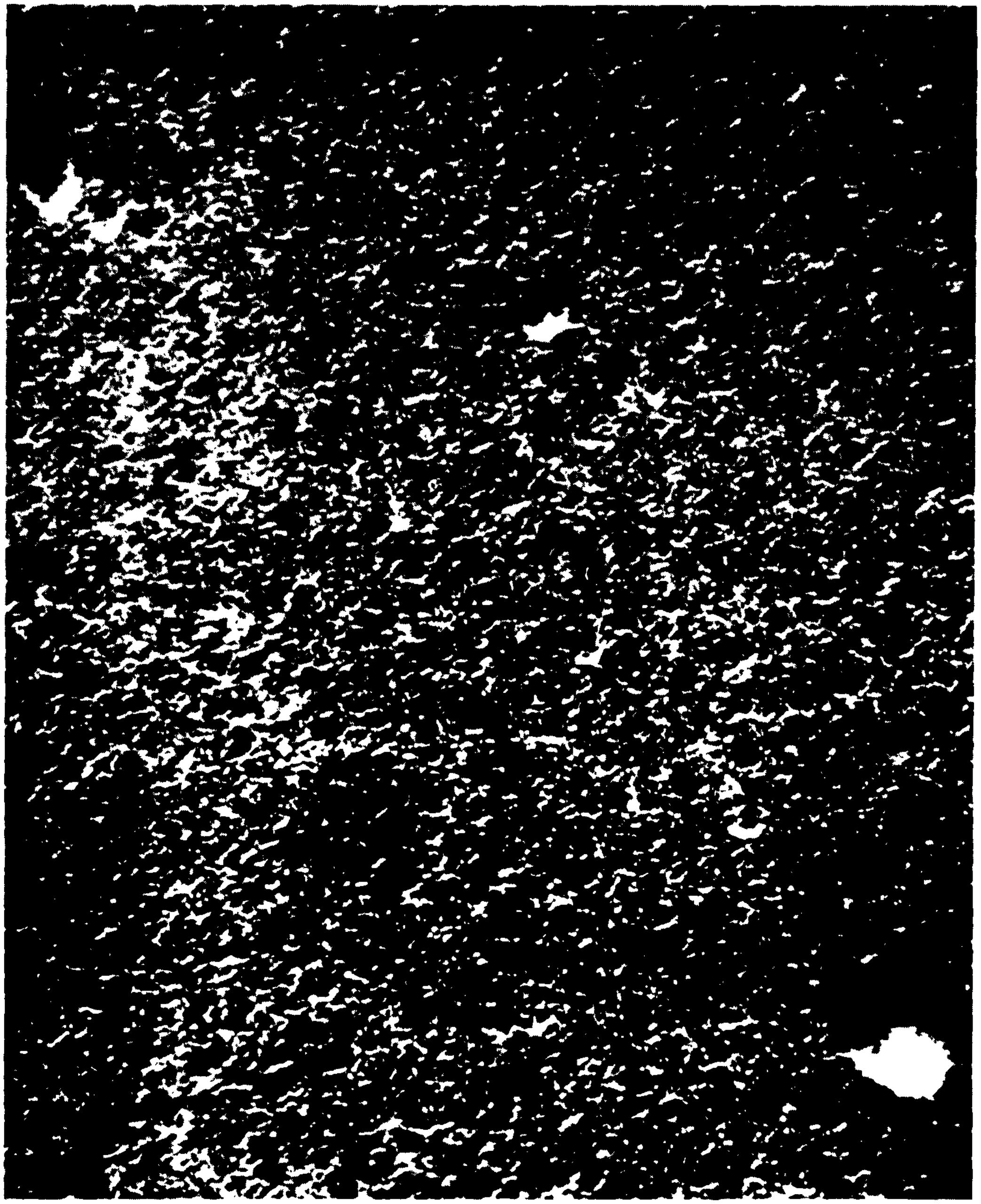

FIGURE 11 CHEMICALLY POLISHED GERMANIUM SURFACE (x 80,000)

D. Experimental Results - Hot Electron Devices

Extensive work has been done at Philco on a Metal Interface Amplifier structure (MIA) which uses an evaporated CdS film as an emitter.[12] This device has exhibited the characteristics of true hot electron action, and was reasonably reproducible and well behaved. Understanding of the structure was limited, however, by a lack of knowledge of the current flow phenomena occurring in metal-insulator-semiconductor systems. Therefore, studies have begun of aluminum-aluminum oxide-cadmium sulfide tunnel emitters. These structures for some reason are not subject to the shorting problem associated with metal-insulator-metal sandwiches, and consequently can provide data on tunneling out of accumulation layers. Experiments are under way on the dependence of these tunneling characteristics on the resistivity of the cadmium sulfide, and the C-V variation versus resistivity. The influence of the substrate on I-V characteristics is also under investigation, since it has been noticed that these sandwiches have lower impedances on glass than on germanium. Quantitative data on these diodes should be available in the next report.

Thin film triode work during this quarter has centered about the metal-oxide-semiconductor diode. One structure which has shown slight active behavior uses an aluminum base sandwiched between oxide-CdS layers on each side. The common emitter parameters of one such structure are shown below in Table VII.

TABLE VII

COMMON EMITTER CHARACTERISTICS
OF THIN FILM TRIODE

Parameter	Value
h_{11}	1.5×10^3 ohms
h_{22}	0.67×10^{-3} mhos $= 1/1.5 \times 10^3$ ohms
h_{21}	0.6
h_{12}	< 0.03

Again, the lack of understanding of the basic diode used in this device prevents immediate development of this structure.

E. Equipment

An Ultek ultra-high vacuum system was received during this quarter, and evaluated for use on this program. The manufacturer's specifications (pressures less than 5 x 10^{-9} torr in less than 4 hours without bakeout) are being met. Furthermore, the system holds vacuum for a fantastically long time. If the chamber is evacuated to 5 x 10^{-9} torr, and the valve separating the ion pump from the "Boostevac" pump and the bell jar then closed, the bell jar pressure will remain below 10^{-7} torr for more than three days. This can only be explained by postulating continued pumping by the evaporated titanium layer on the walls of the "Boostevac" well. In any event, it provides much greater flexibility in device fabrication.

In general, evaporations can be carried out in this system without complication, using standard tungsten filament sources. The most notable exception occurs during the evaporation of aluminum, when bell jar pressure is observed to rise by two orders of magnitude, although the tungsten filament is prebaked at 10^{-6} torr. This may be due to occluded hydrogen in the aluminum charge; tests are underway to verify this with a mass spectrometer capable of detecting partial pressures in the 10^{-10} torr range of materials up to mass 80.

In addition to the above mentioned system, a conventional C. V. C. oil-pumped evaporation system was obtained during this quarter, and considerable effort was spent in rehabilitating it. This system will now meet its specifications of 5 x 10^{-6} torr, and will be used in the study of the natural oxides of aluminum.

SECTION V

CONCLUSIONS

Simple metal-insulator interfaces will probably not be efficient enough to use as collectors in hot electron devices. More sophisticated collectors; e.g., graded-gap materials, may improve collection efficiencies substantially.

There is insufficient knowledge of the natural oxide of aluminum to allow its use as the spacer in the MEA device. Evaporated insulators will be tried for these devices until more is known about $A\ell_2O_3$.

SECTION VI

PLANS FOR NEXT QUARTER

The effect of employing graded gap collector interfaces on the theoretical collection efficiency of hot electron devices will be examined.

Attempts will be made to show the feasibility of using evaporated insulators as the spacers in MEA devices.

Tunneling in metal-insulator-semiconductor diodes will be studied by determining the effect of resistivity of the semiconductor on the I-V and C-V characteristics.

The structure and properties of the natural oxide of aluminum will be examined to determine the origin of the severe shorting problem encountered in MEA devices.

SECTION VII

REFERENCES

1. Mead, Proc. IRE, Vol. 48, No. 3, p. 359, March 1960.
2. Spratt, Schwarz, and Kane, Phys. Rev. Letters, Vol. 6, No. 7, p. 341, April 1, 1961.
3. Schwarz and Spratt, Proc. IRE, Vol. 50, No. 4, p. 467, April 1962.
4. Quinn, Phys. Rev., Vol. 126, No. 4, p. 1453, May 15, 1962.
5. Berman, unpublished Philco Report.
6. Spitzer, Crowell, and Atalla, Phys. Rev. Letters, Vol. 8, pp. 57-58, January 15, 1962.
7. Geppert, Proc. IRE, Vol. 50, No. 6, Part 1, p. 1527, June 1962.
8. Geppert, Solid State Device Research Conference, Univ. of New Hampshire, July 1962.
9. Kahng, Solid State Device Research Conference, Univ. of New Hampshire, July 1962.
10. R. F. Schwarz, Philco Report R. M. 18, April 21, 1961.
11. Fowler and Nordheim, Proc. Roy. Soc. A, Vol. 119, p. 173, 1928.
12. Spratt and Witt, Solid State Device Research Conference, Univ. of New Hampshire, July 1962.
13. Kahng, Proc. IRE, Vol. 50, No. 6, Part 1, p. 1534, June 1962.
14. Schwarz and Spratt, Proc. IRE, Vol. 50.
15. Hall, Solid State Electronics, Vol. 3, p. 320, 1961.
16. Shockley, Solid State Electronics, Vol. 2, p. 35, 1961.

17. Hall, Racette, and Ehrenreich, Phys. Rev. Letters, Vol. 4, p. 456, 1960.

18. Hunter and Fowle, Jour. Electrochem. Soc., Vol. 103, p. 482, September 1956.

19. W. Walkenhorst, Zeit. Techn. Physik, Vol. 22, p. 14, 1941.

20. Cabrera, Terrien, and Haman, Compt. Rend., Vol. 224, p. 1558, 1947.

21. Berning, Hass, and Madden, J. O. S. A., Vol. 50, No. 6, p. 586, June 1960.

22. C. Kirk, Solid State Research Report No. 2, Lincoln Lab., M. I. T., p. 55, 1962.

PHILCO CORPORATION

A SUBSIDIARY OF Ford Motor Company

SCIENTIFIC LABORATORY • Blue Bell, Pennsylvania

Mitchell 6-9100

February 13, 1963

Commander
Armed Services Technical Information Agency
Arlington Hall Station
Arlington, Virginia

Attention:

Subject: Contract DA-49-186-ORD-1056, Philco H-9046
First Quarterly Report Approved

Enclosure: (1) First Quarterly Report (1 Copy)

Gentlemen:

We are forwarding herewith, as enclosure (1), the subject report in accordance with the distribution instructions of the subject contract.

Very truly yours,

PHILCO CORPORATION
Scientific Laboratory

Samuel Murphy
Samuel Murphy
Contract Representative